NASA/TP—2001–211041

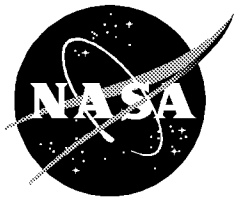

Numerical Simulation of Delamination Growth in Composite Materials

P. P. Camanho
University of Porto, Porto, Portugal

C. G. Dávila and D. R. Ambur
Langley Research Center, Hampton, Virginia

August 2001

The NASA STI Program Office ... in Profile

Since its founding, NASA has been dedicated to the advancement of aeronautics and space science. The NASA Scientific and Technical Information (STI) Program Office plays a key part in helping NASA maintain this important role.

The NASA STI Program Office is operated by Langley Research Center, the lead center for NASA's scientific and technical information. The NASA STI Program Office provides access to the NASA STI Database, the largest collection of aeronautical and space science STI in the world. The Program Office is also NASA's institutional mechanism for disseminating the results of its research and development activities. These results are published by NASA in the NASA STI Report Series, which includes the following report types:

- TECHNICAL PUBLICATION. Reports of completed research or a major significant phase of research that present the results of NASA programs and include extensive data or theoretical analysis. Includes compilations of significant scientific and technical data and information deemed to be of continuing reference value. NASA counterpart of peer-reviewed formal professional papers, but having less stringent limitations on manuscript length and extent of graphic presentations.

- TECHNICAL MEMORANDUM. Scientific and technical findings that are preliminary or of specialized interest, e.g., quick release reports, working papers, and bibliographies that contain minimal annotation. Does not contain extensive analysis.

- CONTRACTOR REPORT. Scientific and technical findings by NASA-sponsored contractors and grantees.

- CONFERENCE PUBLICATION. Collected papers from scientific and technical conferences, symposia, seminars, or other meetings sponsored or co-sponsored by NASA.

- SPECIAL PUBLICATION. Scientific, technical, or historical information from NASA programs, projects, and missions, often concerned with subjects having substantial public interest.

- TECHNICAL TRANSLATION. English-language translations of foreign scientific and technical material pertinent to NASA's mission.

Specialized services that complement the STI Program Office's diverse offerings include creating custom thesauri, building customized databases, organizing and publishing research results ... even providing videos.

For more information about the NASA STI Program Office, see the following:

- Access the NASA STI Program Home Page at ***http://www.sti.nasa.gov***

- E-mail your question via the Internet to help@sti.nasa.gov

- Fax your question to the NASA STI Help Desk at (301) 621-0134

- Phone the NASA STI Help Desk at (301) 621-0390

- Write to:
  NASA STI Help Desk
  NASA Center for AeroSpace Information
  7121 Standard Drive
  Hanover, MD 21076-1320

NASA/TP—2001–211041

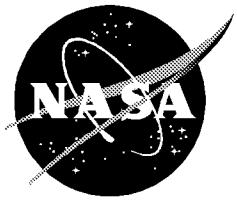

Numerical Simulation of Delamination Growth in Composite Materials

P. P. Camanho
University of Porto, Porto, Portugal

C. G. Dávila and D. R. Ambur
Langley Research Center, Hampton, Virginia

National Aeronautics and
Space Administration

Langley Research Center
Hampton, Virginia 23681-2199

August 2001

Acknowledgments

The first author wishes to acknowledge the Mechanics and Durability Branch, NASA Langley Research Center, for the invitation to collaborate in the Branch's research activities as a Visiting Scientist.

Available from:

NASA Center for AeroSpace Information (CASI)
7121 Standard Drive
Hanover, MD 21076-1320
(301) 621-0390

National Technical Information Service (NTIS)
5285 Port Royal Road
Springfield, VA 22161-2171
(703) 605-6000

Abstract

The use of decohesion elements for the simulation of delamination in composite materials is reviewed. The test methods available to measure the interfacial fracture toughness used in the formulation of decohesion elements are described initially. After a brief presentation of the virtual crack closure technique, the technique most widely used to simulate delamination growth, the formulation of interfacial decohesion elements is described. Problems related with decohesion element constitutive equations, mixed-mode crack growth, element numerical integration and solution procedures are discussed. Based on these investigations, it is concluded that the use of interfacial decohesion elements is a promising technique that avoids the need for a pre-existing crack and pre-defined crack paths, and that these elements can be used to simulate both delamination onset and growth.

Introduction

The fracture process of high performance composite laminates is quite complex, involving both intralaminar damage mechanisms (e.g. matrix cracking, fiber fracture) and interlaminar damage (delamination). An example of a failure with interactive modes is illustrated in Figure 1. Although some progress has been made lately in the development of accurate analytical tools for the prediction of intralaminar damage growth, similar tools for delamination are still not available, and thus delamination is generally not considered in damage growth analyses. Without the delamination failure mode, the predictive capabilities of progressive failure analyses will remain limited.

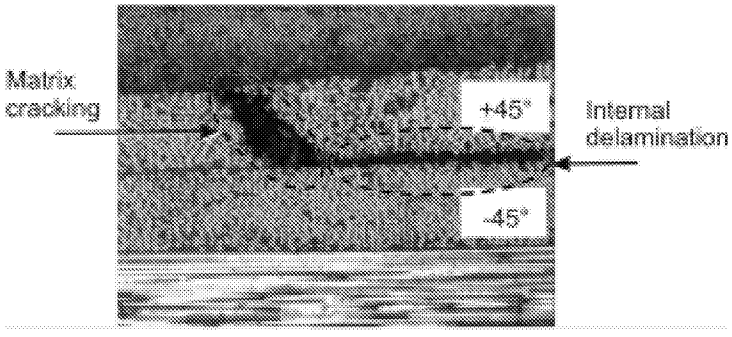

Figure 1. Interaction between intralaminar and interlaminar damage mechanisms [1].

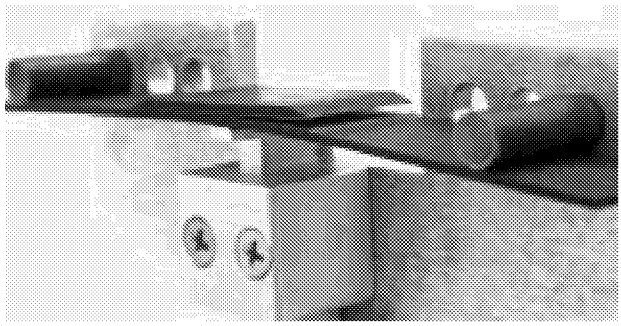

Figure 2. Experiment illustrating stiffener-flange debonding.

Delamination is one of the predominant forms of failure in laminated composites due to the lack of reinforcement in the thickness direction. Delamination as a result of impact or a manufacturing defect can cause a significant reduction in the compressive load-carrying capacity of a structure. The stress gradients that occur near geometric discontinuities such as ply drop-offs, stiffener terminations, skin-stiffener flange interfaces (Figure 2), bonded and bolted joints, and access holes promote delamination initiation, trigger intraply damage mechanisms, and can result in a significant loss of structural integrity.

The analysis of delamination is commonly divided into the study of the initiation and the analysis of the propagation of an already initiated area. Delamination initiation analysis is usually based on stresses and use of criteria such as the quadratic interaction of the interlaminar stresses in conjunction with a characteristic distance [2,3]. This distance is a function of specimen geometry and material properties, and its determination always requires extensive testing.

Crack propagation, on the other hand, is usually predicted using the Fracture Mechanics approach. The Fracture Mechanics approach avoids the difficulties associated with the stress singularity at a crack front but requires the presence of a pre-existing delamination whose exact location may be difficult to determine. When used in isolation, neither the strength-based approach nor the Fracture Mechanics approach is adequate for a comprehensive analysis of progressive delamination failure.

The objective of this report is to examine the several aspects of simulating the delamination, including a method that combines elements of the strength and Fracture Mechanics approaches. A description of test methods that have been proposed to obtain the required material properties is presented. The use of the virtual crack closure technique and interfacial decohesion elements for the simulation of delamination failure is discussed. The main problems associated with the formulation and implementation of interfacial decohesion elements in a finite element model are presented.

Measurement of Interfacial Fracture Toughness

It is essential for developers of computational methods to initiate the analysis with a careful observation of the process to be simulated. In the particular case of delamination growth, it is considered that experimental observation of the physical mechanisms occurring at the interfaces during crack growth provides essential information for the simulation of the process.

The different test methods used for the determination of interlaminar fracture toughness provide an effective means to observe the damaged surfaces under different loading conditions. A careful examination of the characteristics of each test method is required to define the appropriate information to be used in the numerical models.

Mode I

The geometry used to determine the interlaminar fracture toughness in Mode I (G_{IC}) is the double-cantilever beam (DCB) specimen. This specimen is made of a unidirectional fiber-reinforced laminate containing a thin insert at the mid-plane near the loaded end (Figure 3).

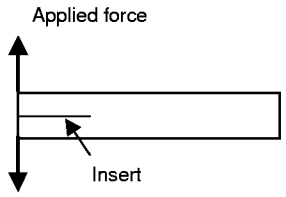

Figure 3. DCB test specimen.

Davies et al. [4] suggested that the major problems associated with this test are the occurrence of fiber bridging across the crack as the crack moves above and below bundles of fibers and the fact that the R-curves associated with this phenomenon are not intrinsic material properties, but they frequently depend on specimen stiffness. However, O'Brien [5] noted that fiber bridging, and consequently the R-curve effect shown in Figure 4, are artifacts of the unidirectional DCB specimen and do not occur in structural composite laminates.

The most appropriate load introduction mechanism, the film thickness of the insert and the data reduction methods for calculating G_{IC} values were proposed as a result of a comprehensive round-robin test program [6]. Although the standard test method limits the DCB specimens to unidirectional (0^o) laminates, it is expected that delaminations in composite structures preferentially arise on interfaces between layers with different orientations. Hence, it is important to have experimental information concerning interlaminar fracture toughness for interfaces between other than 0^o plies. Preliminary results have shown that unidirectional composites provide the most conservative values for G_{IC} [4].

The main problem associated with performing DCB tests on interfaces other than $0^o/0^o$ is that the delamination branches to interfaces away from the midplane [6-8]. Experimental results [7, 8] have shown higher values of G_{IC} for interfaces other than $0^o/0^o$. However, in all of the tests in Refs. 7 and 8 crack jumping was observed and the data was analyzed using standard procedures. This phenomenon has three consequences: firstly, the fracture energy reported is affected by the intralaminar fracture toughness due to the intralaminar matrix cracks. Secondly, as the crack moves from one interface to another, the stiffness of the laminates above and below the crack changes, and this effect should be taken into account in the expressions used to determine G_{IC}. Finally, a DCB test using arms with unequal bending stiffness will also promote Mode II loading [9].

The modified DCB, a new test method designed to overcome these problems, has been proposed by Robinson and Song [10]. Investigations using $[-45^o/0^o/(45^o)_2/0^o/-45^o/45^o/0^o/(-45^o)_2/0^o/45^o)]_s$, $[-45^o/0^o/(45^o)_2/0^o/-45^o/45^o/0^o/(-45^o)_2/0^o/45^o)]_2$ and $[-45^o/45^o/(0^o)_2/45^o/-45^o/45^o/-45^o/(0^o)_2/-45^o/45^o)]_2$ edge delaminated specimens to determine fracture toughness at $+45^o/-45^o$ and $+45^o/+45^o$ interfaces have shown a suppression of the crack jumping that occurs in the conventional DCB specimen. Preliminary tests [10] have also resulted in significantly higher values of G_{IC} for multidirectional laminates compared with unidirectional laminates.

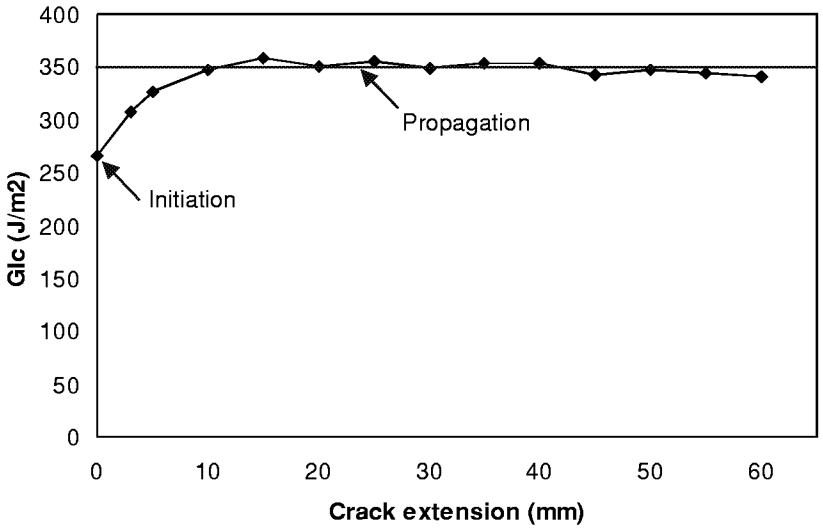

Figure 4. R-curve effect on a DCB test of a $(0^o)_{24}$ CFRP laminate [7].

Mode II

There are four test specimens being considered for the measurement of interlaminar fracture toughnesses under Mode II loading [4, 5]: the end notched flexure specimen (ENF), the stabilized end notched flexure specimen (SENF), the four point end notched flexure specimen (4ENF), and the end loaded split specimen (ELS). Although the ENF test specimen (Figure 5) has received the most attention, it has problems associated with the unstable crack propagation for short crack lengths. One way to stabilize the ENF test is by feedback load control of the test machine [4, 11].

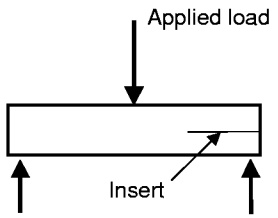

Figure 5. ENF test specimen.

According to Davies [4], the main problems associated with Mode II testing are the definition of the type of starter defect, the definition of crack initiation, the stability of the test, frictional effects on the crack faces and the data analysis. Furthermore, the Mode II fracture toughness is typically much higher and has more scatter than the Mode I fracture toughness [12]: for epoxy matrix composites the G_{IIC}/G_{IC} ratios typically exceed a value of 2.

Observing the fracture surfaces that formed under Mode I and Mode II, O'Brien [12] concluded that under Mode II loading the fracture surface exhibits a rough fracture plane, including 'hackles' (Figure 6), whereas the Mode I fracture surface has a clean cleavage plane. O'Brien also concluded that for both composite laminates and structural elements, failure occurs at a location where Mode I accounts for at least half of the total G at failure, so Mode I and mixed-mode interlaminar fracture toughnesses are the most relevant for predicting delamination failure.

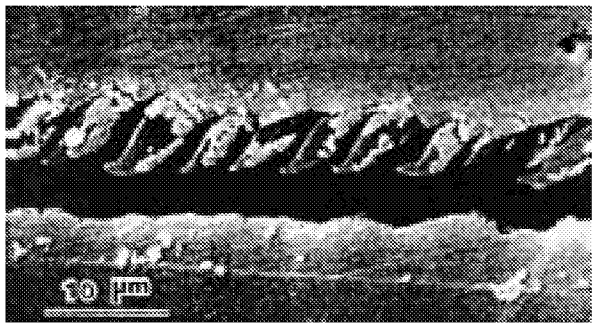

Figure 6. Microcracks forming the shear fracture surface [13].

Mode III

The majority of the research on the determination of interlaminar fracture toughness has been performed for Mode I and Mode II loading. For a complete characterization of the fracture process, Mode III delamination tests are also required.

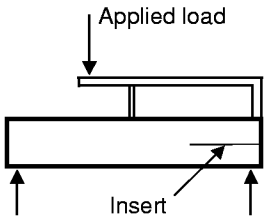

Figure 7. MMB test specimen.

A test that has received much interest is the edge crack torsion (ECT), which is based on the out-of-plane torsion of a cracked $(90^{o}/(\pm 45^{o})_{n}/(\mp 45^{o})_{n}/90^{o})_{s}$ specimen [14]. According to Davies [4], the same concerns occurring in Mode II loading regarding type of defect, initiation definition, and friction need to be addressed for the ECT specimen. Furthermore, the twist-bending coupling due to the presence of off-axis plies leads to a Mode II contribution to the total strain energy release rate that needs to be identified [15]. Using a shear deformation theory, Li and Wang [16] have shown that the Mode II contribution to the total strain energy release rate was negligible.

The influence of the transverse shear modulus G_{23} on the Mode III toughness was investigated by Li and O'Brien [15]. G_{23} is required for the analysis [16] and it is difficult to determine experimentally. It was concluded that a higher value of G_{23} yields lower Mode III toughness estimations and that assuming G_{23} to be equal to G_{12} results in a conservative estimate for the initial delamination length.

Mixed-Mode I and II

The most widely used specimen for mixed-mode fracture is the mixed-mode bending (MMB) specimen, shown in Figure 7, which was proposed by Reeder and Crews [17]. This specimen was later re-designed to minimize geometric nonlinearities [18].

According to Davies [4], the main advantages of the MMB test method are the possibility of using virtually the same specimen geometry for Mode I tests and varying the mixed mode ratio from pure Mode I to pure Mode II.

Numerical Simulation of Delamination

Virtual Crack Closure Technique

The virtual crack closure technique (VCCT) proposed by Rybicki and Kanninen [19] has been used to predict delamination growth in composite materials. This technique is based on Irwin's assumption that when a crack extends by a small amount, the energy absorbed in the process is equal to the work required to close the crack to its original length. The energy release rates can then be computed from the nodal forces and displacements obtained from a finite element model.

The approach can be computationally effective when sufficiently refined meshes are used and when all the elements at the crack tip have the same dimensions in the crack growth direction. Under these conditions, the energy release rates can be obtained from only one analysis.

Köning et al. [20] have used the VCCT to predict delamination growth in plates containing a circular delamination of 10-mm diameter and loaded in tension and compression. A three-dimensional layered element with eight nodes was used and the Mode I, Mode II, and Mode III energy release rates were computed along the delamination front. The location of maximum predicted energy release rates, and hence the delamination growth, were in good agreement with experimental results.

The use of three-dimensional elements to determine energy release rates using the VCCT can overcome the dependence of the results on element shear deformation assumptions. However, these elements lead to computationally intensive models. In order to minimize this problem, Krueger [21] has proposed combining shell and three-dimensional elements. In this approach, the solid three-dimensional elements are used in the immediate vicinity of the delamination front. The connection between the shell and the three-dimensional elements was performed by enforcing the appropriate translations and rotations at the interface. The procedure was used in the simulation of DCB, ENF and single leg bending (SLB) specimens for delaminations located at 0º/0º and +30º/-30º interfaces.

The results of the DCB specimen test clearly show a higher energy release rate at the center of the 0º/0º specimen compared to the specimen edges due to the anticlastic bending effect. This effect was even more pronounced in the specimens containing +30º/-30º interfaces due to the lower bending stiffness of its arms.

The G_{II} values for the ENF specimens are constant across most of the specimen width with higher values in the vicinity of the edges, accompanied by a localized Mode III contribution. The accuracy of the analysis depends on the size of the region modeled with three-dimensional elements: results similar to the ones from a full three-dimensional analysis were obtained with the local zone extended to three times the specimen thickness [21]. Furthermore, for refined meshes, 8-node brick elements combined with 4-node shell elements provided identical results to a model with 20-node brick elements combined with 8-node shell elements. However, care must be taken when simulating the specimen with +30º/-30º interfaces, since experimental results obtained for interfaces other than 0º/0º have shown delamination jumping from one interface to another [7], and the procedure proposed is unable to take this effect into consideration.

The VCCT has also been used to determine energy release rates for delaminations originating from matrix cracks in skin-stringer interfaces when subjected to arbitrary load conditions [22]. Using 8-node plane strain elements with reduced integration, a G versus delamination length a relation was obtained. From these results, it was possible to obtain information concerning the stability of delamination growth.

Care must be taken in selecting the element size at the crack tip when using the VCCT to simulate delamination. Raju et al. [23] have shown that the individual components of the energy release rate does not converge when the ratio of the size of delamination tip element to the ply thickness decreases. This effect does not occur for the total energy release rate, and it is due to the oscillatory part of the stress

singularity occurring in cracks between dissimilar media. It was shown that when using delamination tip elements with a size of one-quarter to one-half of the ply thickness, the individual components obtained agreed well with the results from a model that had a resin-rich layer incorporated between the plies [23].

Although providing valuable information concerning onset and stability of delamination growth, the use of VCCT to simulate delamination growth requires complex moving mesh techniques [24] to advance the crack front when the local energy release rate exceeds a critical value. Furthermore, an initial delamination must be defined and, for certain geometries and load cases, the location of the delamination front might be difficult to determine.

Interfacial Decohesion Elements

One approach to overcome the above limitations of the VCCT is the use of interfacial decohesion elements placed between the composite material layers. Interfacial decohesion elements combine a stress based formulation with a Fracture Mechanics based formulation and are used to define the non-linear constitutive law of the material at the interface between laminae.

The concept of decohesion elements is based on a Dugdale-Barenblatt type cohesive zone [25, 26] and was first applied to the analysis of concrete cracking by Hillerborg et al. [27]. The concept of cohesive zone models has also been used by Needleman [28] to describe the process of void nucleation from inclusions, to simulate fast crack growth in brittle solids [29], and for intersonic crack growth under shear loading [30].

Needleman [28] considered cohesive zone models particularly attractive when interfacial strengths are relatively weak compared with the adjoining material, as in the case of composite laminates. The proposed constitutive equations for the interface are phenomenological mechanical relations between the tractions and interfacial separations such that, with increasing interfacial separation, the tractions across the interface reaches a maximum, decreases and vanishes when complete decohesion occurs, as illustrated in Figure 8.

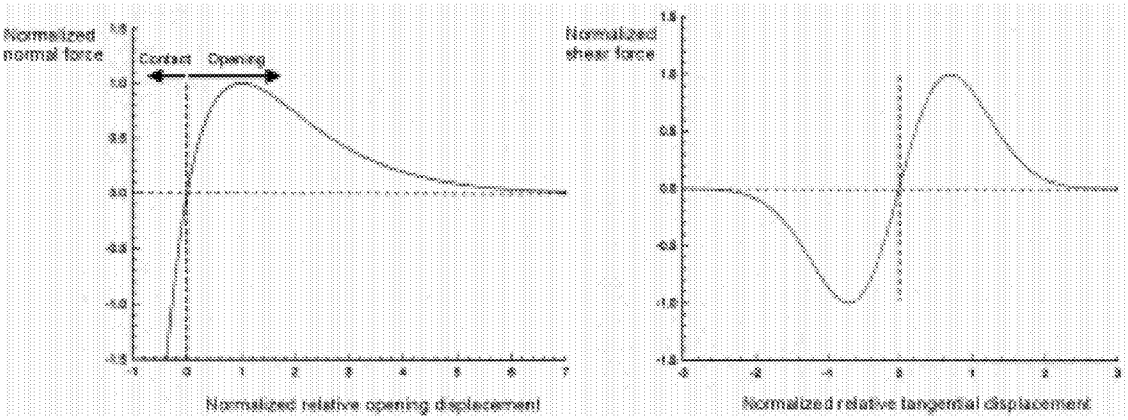

Figure 8. Normal and shear tractions across the cohesive surface as a function of relative displacements [29].

The decohesion response was specified in terms of a potential relating the interfacial tractions and the relative tangential and normal displacements across the interface [29]. The resulting work of normal separation and tangential separation can be related to the critical values of energy release rates.

In fact, the cohesive zone formulation is identical to Griffith's theory of fracture: considering the integral *J* proposed by Rice [31]:

$$J = \int_{\Gamma} (wdy - \mathrm{T}.\frac{\partial \mathrm{u}}{\partial x} ds) \tag{1}$$

where Γ is any contour surrounding the notch tip, $\boldsymbol{u}$ is the displacement vector, $\boldsymbol{T}$ is the traction vector defined accordingly to the outward normal along Γ, and w is the strain energy density. Evaluating the integral *J* on the contour Γ defined by the cohesive zone (Figure 9):

$$J = \int_{\Gamma} (wdy - \sigma(\delta) \frac{d\delta}{dx} dx) \tag{2}$$

Taking into account that $dy=0$ along the selected contour [31]:

$$J = -\int_{\Gamma} (\sigma(\delta) \frac{d\delta}{dx} dx) = -\int_{\Gamma} \frac{d}{dx} (\int_0^{\delta} \sigma(\delta) d\delta) dx = \int_0^{\delta_t} \sigma(\delta) d\delta \tag{3}$$

where δ_t is the relative displacement at the crack tip.

It has been shown that, for self-similar crack growth and negligible cohesive zones (or small-scale yielding), the *J*-integral can be expressed as the rate of decrease of potential energy with respect to the crack length and is equivalent to the energy release rate, *G* [31], [32]:

$$J = -\frac{\partial \Pi}{\partial a} = G \tag{4}$$

where Π is the potential energy of the system. From (3) and (4):

$$G = \int_0^{\delta_t} \sigma(\delta) d\delta \tag{5}$$

Considering $\delta_t = \delta_{max}$ at crack extension the critical value of *G*, G_c, is:

$$G_C = \int_0^{\delta_{max}} \sigma(\delta)\, d\delta \tag{6}$$

When using Barenblatt's [26] model in the simulation of delamination growth, the cohesive zone can still transfer load after delamination onset (point 3 in Figure 9), until the critical value of the energy release rate is attained (point 4 in Figure 9).

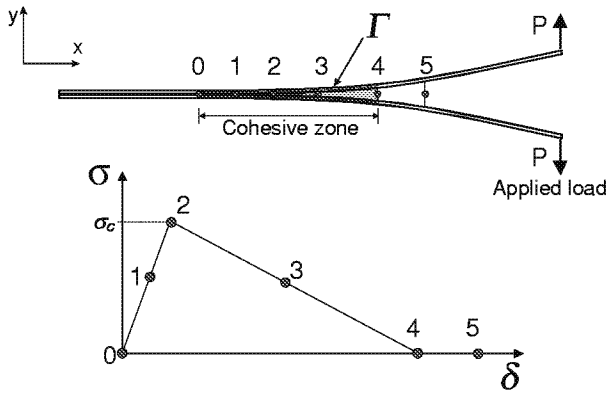

Figure 9. Cohesive zone ahead of delamination tip.

The concept of decohesion zones to simulate delamination growth in composites is usually implemented by means of decohesion elements connecting the individual plies of a composite laminate. These elements can model the discontinuity introduced by the growth of delaminations. Decohesion elements use a high penalty stiffness before delamination onset to prevent additional deformations (see point 1 in Figure 9).

Decohesion elements can be divided into two main groups: continuous decohesion elements and point decohesion elements. Several types of continuous decohesion elements have been proposed, ranging from plane decohesion elements with zero thickness connecting solid elements [33-36]; plane decohesion elements with finite thickness connecting shell elements [37]; and line decohesion elements [38-40]. Point decohesion elements are identical to spring elements connecting nodes [41, 42].

The concept of decohesion elements has been used in different types of problems: compression-after-impact [33, 35], stiffener-flange debonding [36], damage growth from discontinuous plies [40], diametrical compression of composite cylinders [37]. The use of decohesion elements in the simulation of delamination growth in compression-after-impact problems is illustrated in Figures 10 and 11. Figure 10 shows the deformed shape of a CFRP laminate containing a delamination. Figure 11 shows the initial delamination due to the impact load and its predicted propagation. Figure 11 indicates that decohesion elements can capture non-self-similar crack growth.

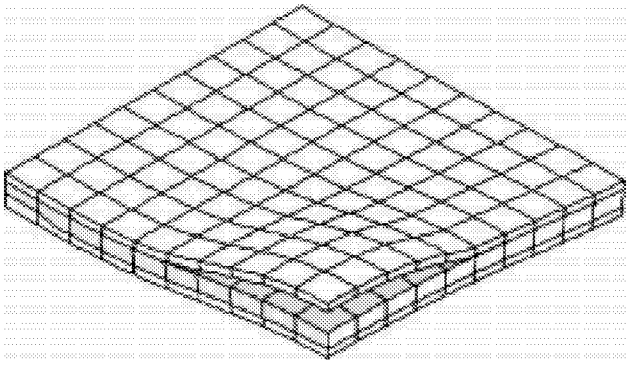

Figure 10. Global buckling in a $[0^{o}_{4}/90^{o}_{4}]$ CFRP laminate under compression-after-impact loading [35].

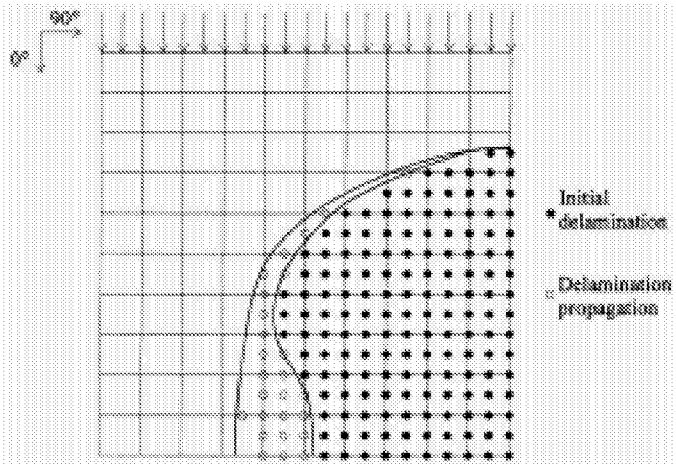

Figure 11. Delamination propagation for a ($0^{o}_{4}/90^{o}_{4}$) CFRP laminated composite under compression-after-impact loading [35].

The following issues must be addressed in order to obtain accurate results for the simulation of delamination using interfacial decohesion elements.

Constitutive Equations

The need for an appropriate constitutive equation in the formulation of the decohesion element is fundamental for an accurate simulation of the interlaminar cracking process. In addition to Needleman's [28-30] interfacial behavior represented in Figure 8, other constitutive equations proposed are [43]: linear elastic-perfectly plastic, linear elastic-linear softening, linear elastic-progressive softening, linear elastic-regressive softening (Figure 12).

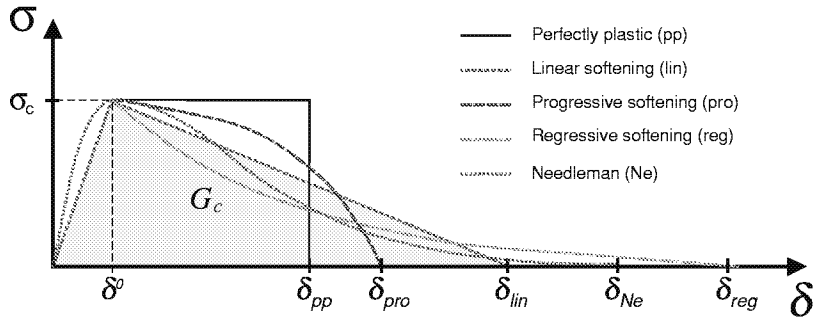

Figure 12. Constitutive strain softening equations [43].

In order to simulate the cohesive zone process ahead of the crack tip represented in Figure 9, a linear elastic-linear softening behavior is usually implemented [33-39, 44-46]. A high initial stiffness is used to hold the top and bottom faces of the decohesion element together in the linear elastic range. For pure Mode I, II or III loading, after the interfacial normal or shear tractions attain their respective interlaminar tensile or shear strengths, the stiffnesses are gradually reduced to zero. The area under the stress-relative displacement curves is the respective (Mode I, II or III) fracture energy (see equation 6 and Figure 13).

$$\int_0^{\delta_{\max,3}} \sigma_{33}(\delta) d\delta_3 = G_{IC} \tag{7}$$

$$\int_0^{\delta_{\max,2}} \tau_{13}(\delta) d\delta_2 = G_{IIC} \tag{8}$$

$$\int_0^{\delta_{\max,1}} \tau_{23}(\delta) d\delta_1 = G_{IIIC} \tag{9}$$

Therefore, the properties required to define the interfacial behavior are the initial stiffness (or penalty stiffness), K_P, the corresponding fracture energies, G_{IC}, G_{IIC} and G_{IIIC} and the corresponding interlaminar tensile or shear strengths, $\overline{\sigma}_{33}$, $\overline{\tau}_{13}$ and $\overline{\tau}_{23}$.

Once a crack is unable to transfer any further load (point 5 in Figure 9), all the penalty stiffnesses revert to zero. However, it is necessary to avoid the interpenetration of the crack faces. Therefore, the contact problem is addressed by re-applying the normal penalty stiffness when interpenetration is detected. The contact condition is related to the constitutive relation proposed by Needleman [28] and shown in Figure 8.

This interfacial constitutive equation, which is shown in Figure 13, can be implemented as follows:

i) *For* $\delta_i < \delta_{0,i}$, the constitutive equation is given by:

$$\boldsymbol{\sigma} = \begin{bmatrix} K_P & 0 & 0 \\ 0 & K_P & 0 \\ 0 & 0 & K_P \end{bmatrix} \boldsymbol{\delta} = \boldsymbol{D\delta} \tag{10}$$

ii) *For* $\delta_{0,i} \le \delta_i < \delta_{max,i}$, the constitutive equation is given by:

$$\boldsymbol{\sigma} = (\boldsymbol{I} - \boldsymbol{E})\boldsymbol{D\delta} \tag{11}$$

where $\boldsymbol{I}$ is the identity matrix and $\boldsymbol{E}$ is a diagonal matrix defining the position of the integration point in the softening curve.

iii) *For* $\delta_i \ge \delta_{max,i}$, all the penalty stiffnesses revert to zero. Interpenetration is prevented by reapplying only the normal stiffness if crack closure is detected, meaning that frictional effects are neglected.

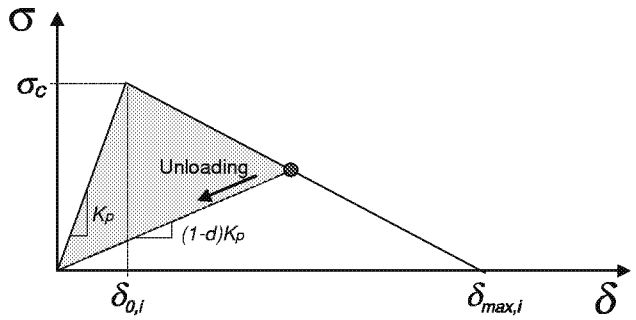

Figure 13. Bi-linear constitutive equation.

The process of reapplying the normal stiffness when interpenetration is detected is typical of solution procedures of contact problems using penalty methods in a constrained variational formulation. It is also clear from this formulation that the accuracy of the analysis depends on the penalty stiffness K_P chosen

for the linear-elastic region of the constitutive equation. High values of K_P will avoid interpenetration of the crack faces but can lead to numerical problems.

Some authors have determined the value for the penalty stiffness as a function of the interface properties. Daudeville et al. [47], for instance, have considered the interface as a resin rich zone of small thickness, e_i, and have proposed a penalty stiffnesses defined as:

$$K_P^I = \frac{E_3}{e_i}; K_P^{II} = \frac{2G_{13}}{e_i}; K_P^{III} = \frac{2G_{23}}{e_i} \tag{12}$$

where G_{23}, G_{13}, and E_3 are the elastic moduli of the resin rich zone. Values that have been calculated for the penalty stiffness K_P include, 5.7x 10^7 N/mm^3 [39], and 10^8 N/mm^3 [44]. Other authors have shown that lower values such as 10^7 N/mm^3 [34] can adequately minimize the relative displacements at the interface while avoiding the potential for numerical errors related to computer precision.

In order to fully define the interfacial behavior, the unloading response must be specified. Crisfield et al. [37, 38] and Daudeville [47] assumed that, with reversing strains, the material unloads directly toward the origin (see Figure13). This procedure seems reasonable since the interfacial stiffness when reloading is lower than the original (undamaged) stiffness. Such a procedure simulates the effects of the previous damage mechanisms that occurred along the interface. Other authors [40] have proposed an unloading curve with a slope corresponding to Hooke's law. Such a procedure, typically used in the formulation of plasticity problems, would lead to the use of the same penalty stiffness when reloading, and to permanent relative displacements along the interface when the load reverts to zero.

Mixed Mode Delamination

In structural applications of composites, delamination growth is more likely to occur under mixed-mode loading. Therefore, a general formulation for decohesion elements should deal with mixed-mode delamination growth problems. O'Brien et al. [12] have proposed using a cubic equation obtained from least square regression curve fit of the experimental data, as shown in Fig. 14.

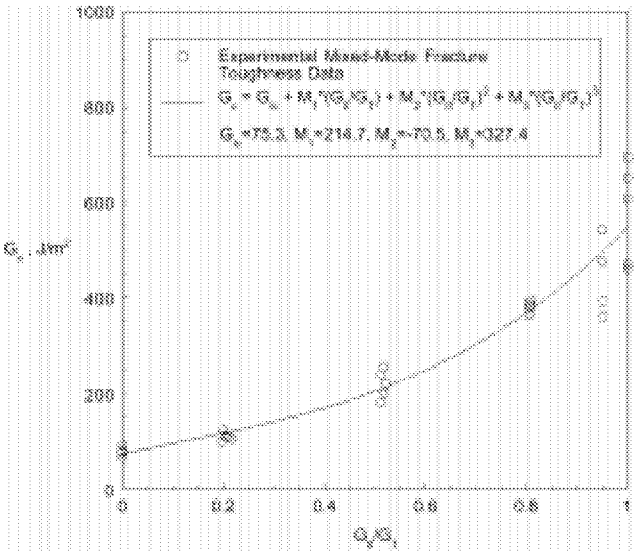

Figure 14. Mixed mode delamination criterion for AS4/3501-6 [12]

The development of a criterion such as shown in Figure 14 requires a more extensive test program than is often available. In the absence of such test data in the mixed-mode range, the analyst must rely on empirical expressions. A comprehensive study of failure criteria for mixed-mode delamination in brittle epoxy, tough epoxy and thermoplastic composites under the full mixed-mode range was performed by Reeder [48, 49]. Some of the criteria evaluated include:

i) Linear Criterion:

$$\left(\frac{G_I}{G_{IC}}\right)+\left(\frac{G_{II}}{G_{IIC}}\right)=1 \tag{13}$$

ii) Power Law Criterion:

$$\left(\frac{G_I}{G_{IC}}\right)^{\alpha}+\left(\frac{G_{II}}{G_{IIC}}\right)^{\beta}=1 \tag{14}$$

iii) Bilinear Criterion:

$$G_I=\xi G_{II}+G_{IC} \tag{15}$$

Mixed-mode bending tests were used to measure the mixed-mode delamination toughness of the above composites, providing experimental data to assess the criteria. The linear model appears to be the most suited to predict failure of thermoplastic PEEK matrix composites because the results were very comparable to the more sophisticated criteria, while using two fewer independent variables. However, the linear criterion was found to be inaccurate for predicting the response of epoxy composites. The proposed bilinear criterion [48], taking into account the modification of failure mechanisms near the one-to-one ratio of G_I/G_{II}, was found to yield the best results when simulating epoxy matrix composites. The power law criterion provides a conservative simulation of delamination in epoxy matrix composites.

Chen et al. [38] have proposed the use of both the linear criterion and the power law criterion to predict total interfacial fracture under mixed-mode loading and obtained a reasonable agreement between predictions and experimental results in the simulation of fixed ratio mixed-mode (FRMM) tests when using $\alpha=\beta=4$. Other authors [34] have used a criterion based on moving damage surfaces as a function of the normal and in-plane relative displacements.

An issue that should also be addressed is the definition of a delamination onset criterion for multiaxial traction states. Under pure Mode I, II or III loading, the onset can be determined simply by comparing the traction components with their respective material allowables. However, under mixed-mode loading this approach must be recast, since delamination onset due to multi-axial traction states may occur before any of the traction components involved reach their respective allowables.

Cui et al. [50] have shown that stress-based criteria can be used for uncracked specimens where there is no macroscopic singularity. Furthermore, the authors have shown that interaction between stress components is important in determining delamination initiation, since poor results were obtained by using the maximum stress criterion [50]. This observation is confirmed by Mohammadi et al. [51], who state that it is widely accepted that the quadratic failure criterion based on interlaminar stresses can be properly used to predict the initiation of delamination.

Element Integration

Special care must be taken in the integration scheme adopted for decohesion finite elements as oscillations of the traction field may occur [34, 39, 44, 45, 52]. Schellekens and de Borst [44, 45] have

demonstrated using eigenmode analysis of the element stiffness matrices that Gaussian integration can cause undesired spurious oscillations of the traction field when large stress gradients are present over an decohesion element. With increasing mesh refinement, the element performance improves due to the decreasing stress gradients.

The authors concluded that for line decohesion elements and linear plane decohesion elements the performance can be improved by using either a nodal lumping scheme, Newton-Cotes, or Lobatto integration scheme. It was shown that the eigenmodes of elements integrated with such techniques do not show coupling between displacements at adjacent nodes [45].

For quadratic decohesion elements, Newton-Cotes and Lobatto integration schemes produce smooth traction profiles when the displacement field over the element varies in only one direction. Oscillatory traction profiles may occur in other cases [52]. However, this adverse effect is only significant for the central integration point, and it is less pronounced than the oscillations occurring when Gauss integration is used. If necessary, more refined meshes or linear elements can be used to reduce the magnitude of the stress oscillation.

Another relevant issue related with the integration of decohesion elements is the use of full integration schemes. Analyses of problems involving crack propagation and strain-softening behavior have shown that the use of full integration was superior to the use of reduced integration schemes [53]. However, Alfano and Crisfield [54] have shown that for fully integrated linear 4-node decohesion elements, increasing the number of Simpson integration points from 2 to 20 results in an increase of spurious oscillations in the load-displacement curve and, consequently, to less a robust solution algorithm.

Non-linear Solution Procedures

The softening nature of the decohesion element constitutive equation causes convergence difficulties in the solution of the Finite Element Analysis. Crisfield et al. [43] found that when using the Newton-Raphson method, under load (with the arc-length method) or displacement control, the iterative solutions often oscillated when a positive slope of the total potential energy was found, and therefore failed to converge. In order to obtain convergence, a 'line search' procedure with a negative step length was proposed.

In a recent work, Mi et al. [39] proposed the use of a modified cylindrical arc-length method [55] to obtain converged solutions. This technique chooses between the alternative roots to the arc-length constraint, selecting the one involving the minimum residual [55]. However, even with this new technique, the solution sometimes enters a cycle and oscillates between two points. The oscillation must be detected so that the increment size can be reduced. It was also found that when coarse meshes are used, a 'snap-back' type of behavior might occur [39]. Therefore, in order to obtain a relatively smooth solution, the mesh should be fine enough to include at least two decohesion elements in the cohesive zone located at the crack tip. This means that for Mode I loading and for a given G_{IC}, the lower the interlaminar tensile strength $\overline{\sigma}_{33}$, the larger will be the cohesive zone, and hence the smoother the solution. This 'root selection' method has also been successfully used by Wisheart and Richardson [46] in the simulation of DCB tests in composite laminates.

In the previously mentioned work, Chen et al. [38] have used two different techniques to obtain converged solutions: displacement control in conjunction with the line searches in the commercial finite element code ABAQUS and the modified cylindrical arc-length method [55] in the LUSAS finite element code. It was found that it is significantly easier to obtain convergence when using linear decohesion elements. A LUSAS model using quadratic elements failed to converge. Similarly, an ABAQUS model with the same interlaminar tensile strength and linear elements also failed to converge. The convergence

difficulties were overcome by reducing the interlaminar tensile strength to 40% of the original value whilst maintaining a constant fracture energy. The improvement in convergence is due to the previously mentioned effect of increasing the cohesive zone ahead of the crack tip. This modification had only an effect on the behavior around the ultimate load of the structure. As expected, when decreasing the interlaminar tensile strength, the predicted peak load also decreased.

The arc-length method proposed by Riks [56] to pass limit points in non-linear problems uses a constraint equation to relate the incremental load factor to the norm of the incremental displacement vector. However, Schellekens [51] recognized that the arc-length method has difficulty converging in problems such as the simulation of delamination using decohesion elements where failure is highly localized. Therefore, the authors suggested that the displacement norm should be determined considering only the dominant degree of freedom, as the definition of a constraint equation based on the global displacement vector is less effective. A nodal crack opening displacement (COD) control was proposed [51] where the load factor is calculated from a reduced displacement vector that is a function of the COD.

Reddy Jr. [37] used explicit time integration to overcome the difficulties of having to deal with material softening and contact conditions when using decohesion elements. Although explicit formulations are typically used to solve transient dynamic problems, they were used to address a problem involving quasi-static loading. The explicit time integration methods are conditionally stable because the minimum time step used for the explicit time integration of the governing equations depends on the highest eigenvalue in the mesh. Estimates for the frequency of the vibrational modes that influence the choice of the stable time increment were performed and it was found that the frequency depends on the penalty parameter K_P. However, this analysis is valid before delamination onset, as it is expected that when the element is softening the minimum time step used for the explicit time integration is constantly being modified.

Ladevèze et al. [57-59] have proposed a 'large time increment method' to solve the nonlinear problem. The procedure is based on a single global iterative procedure on the whole loading history between linear steps and non-linear steps.

Discussion

In order to improve the generality and the accuracy of the formulations described, a number of developments are required. These may include:

- A criterion able to predict delamination onset under multi-axial stresses. The use of mixed-mode criteria to predict total element decohesion is proposed.
- Decohesion element constitutive equation: Experimental results have shown different damage mechanisms under pure Mode I and Mode II loading. However, most of the approaches assume a bi-linear constitutive equation for both loading modes. An investigation of the appropriate constitutive equations for different loading modes, including unloading behavior, is required.
- The development of decohesion elements compatible with plate/shell elements would allow the effective analysis of large-scale structures (e.g. debonding in skin-stiffener).
- Usually, the fracture process of a composite structure occurs by a combination of intralaminar (e.g. matrix transverse cracking, fiber fracture) and interlaminar damage (Figure 1). Therefore, a model incorporating the simulation of the different damage mechanisms would provide a general tool for the failure analysis of a composite structure.
- Point-to-surface contact algorithms such as the one proposed in [34] should be developed to avoid interpenetration of the crack faces after complete decohesion, especially when large tangential relative displacements occur.

Concluding Remarks

The VCCT is a valuable technique for the determination of both delamination growth and the contributions of different loading modes to the global energy release rate. Important information can be obtained without having computationally expensive models, using only interlaminar fracture toughness for delamination propagation prediction, and no stress-based allowable. However, the VCCT must use a pre-defined crack and for some structures/loads the precise location of crack initiation might not be obvious. Furthermore, complex moving-mesh techniques are required to simulate delamination growth.

The use of decohesion elements can overcome some of the above difficulties. Using decohesion elements, both onset and propagation of delamination can be simulated without previous knowledge of crack location and propagation direction.

The material properties required to define the element constitutive equation are the interlaminar fracture toughnesses and the corresponding strengths. The fact that the strengths are required is a disadvantage when compared with the VCCT, which only requires interlaminar fracture toughnesses.

It is also clear that Newton-Cotes integration schemes should be used in the definition of the stiffness matrix of decohesion elements because Gaussian integration may lead to oscillations of the stress field. Due to the localized softening associated with delamination growth, the solution procedures for the nonlinear problem requires special techniques such as the COD control. Such techniques can enhance the numerical stability and, consequently, improve the convergence rate.

References

1. Camanho, P. P., "Application of Numerical Methods to the Strength Prediction of Mechanically Fastened Joints in Composite Laminates," PhD Thesis, Imperial College of Science and Technology, University of London, U.K., 1999.
2. Dávila, C. G. and E. R. Johnson, "Analysis of Delamination Initiation in Postbuckled Dropped-Ply Laminates," *AIAA Journal*, Vol. 31 (4), 1993, pp.721-727.
3. Camanho, P. P. and F. L. Matthews, "Delamination Onset Prediction in Mechanically Fastened Joints in Composite Laminates," *Journal of Composite Materials*, Vol. 33, 1999, pp. 906-27.
4. Davies, P., B. R. K. Blackman, and A. J. Brunner, "Towards Standard Fracture and Fatigue Test Methods for Composite Materials," Proceedings of the 6as Jornadas De Fractura, Sociedade Portuguesa de Materiais, Portugal, 1998, pp. 151-167.
5. O'Brien, T. K., "Interlaminar Fracture Toughness: The Long and Winding Road to Standardisation," *Composites-Part B*, Vol. 29, 1998, pp. 57-62.
6. O'Brien, T. K. and R. H. Martin, "Round Robin Testing for Mode I Interlaminar Fracture Toughness of Composite Materials," *Journal of Composites Technology & Research*, Vol. 15(3), 1993, pp. 269-81.
7. Morais, A. B., A. T. Marques, and P. T. Castro, "Estudo da Aplicação de Ensaios de Fractura Interlaminar de Modo I a Laminados Compósitos Multidireccionais," Proceedings of the 7as Jornadas De Fractura, Sociedade Portuguesa de Materiais, Portugal, 2000, pp. 90-95 (in Portuguese).
8. Choi, N. S., A. J. Kinloch, and J. G. Williams, "Delamination Fracture of Multidirectional Carbon-Fibre Composites Under Mode I, Mode II and Mixed-Mode I/II Loading," *Journal of Composite Materials*, Vol. 33, 1999, pp. 73-100.

9. Williams, J. G. "The Fracture Mechanics of Delamination Tests," *Journal of Strain Analysis*, Vol. 24, 1989, pg. 207.

10. Robinson, P. and D. Q. Song, "A Modified DCB Specimen for Mode I Testing of Multidirectional Laminates," *Journal of Composite Materials*, Vol. 26, 1992, pp. 15-54.

11. Kageyama, K., M. Kikuchi, and N. Yanagisawa, ASTM STP 1110, American Society for Testing and Materials, 1991.

12. O'Brien, T. K., "Composite Interlaminar Shear Fracture Toughness, GIIC: Shear Measurement of Sheer Myth?" ASTM-STP 1330, American Society for Testing and Materials, 1998, pp. 3-18.

13. Corleto, C. R. and W. L. Bradley, "Correspondence Between Stress Fields and Damage Zones Ahead of Crack Tip of Composites under Mode I and Mode II Delamination," Proceedings of the Sixth International Conference on Composite Materials (ICCM-6), Vol. 3, 1993, pp. 378-387.

14. Lee, S. M., "An Edge Crack Torsion Method for Mode III Delamination Fracture Testing," *Journal of Composites Technology & Research*, Vol. 15(3), 1993, pp. 193-201.

15. Li, J., and O'Brien, T. K., "Simplified Data Reduction Methods for the ECT Test for Mode III Interlaminar Fracture Toughness," *Journal of Composites Technology & Research*, Vol. 18(2), 1996, pp. 96-101.

16. Li, J. and Y. Wang, "Analysis of a Symmetric Laminate With Mid-Plane Free Edge Delamination Under Torsion: Theory and Application to the Edge Crack Torsion (ECT) Specimen for Mode III Toughness Characterisation," *Engineering Fracture Mechanics*, Vol. 49(2), 1994, pp. 179-194.

17. Crews, J. H. and J. R. Reeder, "A Mixed-Mode Bending Apparatus for Delamination Testing," NASA TM 100662, 1988.

18. Reeder, J. R. and J. H. Crews, "Nonlinear Analysis and Redesign of the Mixed-Mode Bending Delamination Test," NASA TM 102777, 1991.

19. Rybicki, E. F. and M. F. Kanninen, "A Finite Element Calculation of Stress Intensity Factors by a Modified Crack Closure Integral," *Engineering Fracture Mechanics*, Vol. 9, 1977, pp. 931-938.

20. König, M, R. Krueger, and S. Rinderknecht, "Numerical Simulation of Delamination Buckling and Growth," Proceedings of the 10th International Conference on Composite Materials (ICCM-10), Whistler, Canada, 1995.

21. Krueger, R., and O'Brien, T.K., "A Shell/3D Modeling Technique for the Analysis of Delaminated Composite Laminates," Composites Part A: Applied Science and Manufacturing, Vol. 32(1), 2001, pp. 25-44.

22. Krueger, R., P. J. Minguet, and T. K. O'Brien, "A Method for Calculating Strain Energy Release Rates in Preliminary Design of Composite Skin/Stringer Debonding UnderMulti-Axial Loading," Composite Structures: Theory and Practice, ASTM STP 1383, Nov. 2000, pp. 105-128.

23. Raju, I. S., J. H. Crews, and M. A. Aminpour, "Convergence of Strain Energy Release Rate Components for Edge-Delaminated Composite Laminates," *Engineering Fracture Mechanics* 30(3), 1988, pp. 383-396.

24. Rinderknecht, S. and B. Kroplin, "Calculation of Delamination Growth with Fracture and Damage Mechanics." Recent Developments in Finite Element Analysis, CIMNE, Barcelona, Spain, 1994.

25. Dugdale, D. S., "Yielding of Steel Sheets Containing Slits," *Journal of Mechanics and Physics of Solids*, 8, 1960, pp. 100-104.

26. Barenblatt, G. I., "Mathematical Theory of Equilibrium Cracks in Brittle Failure," *Advances in Applied Mechanics*, Vol. 7, 1962.

27. Hilleborg, A., M. Modeer, and P. E. Petersson, "Analysis of Crack Formation and Crack Growth in Concrete by Fracture Mechanics and Finite Elements," *Cement and Concrete Research*, Vol. 6, 1976, pp. 773-782.

28. Needleman, A. "A Continuum Model for Void Nucleation by Inclusion Debonding," *Journal of Applied Mechanics*, Vol. 54, 1987, pp. 525-531.

29. Xu, X. P. and A. Needleman, "Numerical Simulations of Fast Crack Growth in Brittle Solids," *Journal of Mechanics and Physics of Solids*, Vol. 32(9), 1987, pp. 1397-1434.

30. Needleman, A., "An Analysis of Intersonic Crack Growth Under Shear Loading," *Journal of Applied Mechanics*, Vol. 66, 1999, pp. 847-857.

31. Rice, J. R., "A Path Independent Integral and the Approximate Analysis of Strain Concentration by Notches and Cracks," *Journal of Applied Mechanics*, 1968, pp. 379-386.

32. Gdoutos, E. E., "Fracture Mechanics Criteria and Applications", Kluwer Academic Publishers, Dordrecht, The Netherlands, 1990.

33. de Moura, M. F., J. P. Gonçalves, A. T. Marques, and P. T. Castro, "Modeling Compression Failure After Low Velocity Impact on Laminated Composites Using Interface Elements," *Journal of Composite Materials,* Vol. 31, 1997, pp. 1462-1479.

34. Gonçalves, J. P., M. F. de Moura, P. T. Castro, and A. T. Marques, "Interface Element Including Point-to-Surface Constraints for Three-Dimensional Problems With Damage Propagation," *Engineering Computations*, Vol. 17(1), 2000, pp. 28-47.

35. de Moura, M. F., J. P. Gonçalves, A. T. Marques, and P. T. Castro, "Prediction of Compressive Strength of Carbon-Epoxy Laminates Containing Delaminations by Using a Mixed-Mode Damage Model," *Composite Structures*, Vol. 50, 2000, pp. 151-157.

36. Dávila, C. G., P. P. Camanho, and M. F. de Moura,, "Mixed-Mode Decohesion Elements for Analyses of Progressive Delamination," Proceedings of the 42nd AIAA/ASME/ASCE/AHS/ASC Structures, Structural Dynamics and Materials Conference, Seattle, WA, April 16-19, 2001.

37. Reddy Jr., E. D., F. J. Mello, and T. R. Guess "Modeling the Initiation and Growth of Delaminations in Composite Structures," *Journal of Composite Materials,* Vol. 31, 1997, pp. 812-831.

38. Chen, J., M. A. Crisfield, A. J. Kinloch, E. P. Busso, F. L. Matthews, and Y. Qiu, "Predicting Progressive Delamination of Composite Material Specimens Via Interface Elements," *Mechanics of Composite Materials and Structures,* Vol. 6, 1999, pp. 301-317.

39. Mi, Y., M. A. Crisfield, G. A. O. Davies, and H. B. Hellweg, "Progressive Delamination Using Interface Elements," *Journal of Composite Materials,* Vol. 32, 1998, pp. 1246-1273.

40. Petrossian, Z. and M. R. Wisnom, "Prediction of Delamination Initiation and Growth From Discontinuous Plies Using Interface Elements," *Composites-Part A,* Vol. 29, 1998, pp. 503-515.

41. Cui, W. and M. R. Wisnom, "A Combined Stress-Based and Fracture Mechanics-Based Model for Predicting Delamination in Composites," *Composites,* Vol. 24(6), 1993, pp. 467-474.

42. Shahwan, K. W. and A. M. Waas, "Non-Self-Similar Decohesion Along a Finite Interface of Unilaterally Constrained Delaminations," Proceedings of the Royal Society of London, Vol. 453, 1997, pp. 515-550.

43. Crisfield, M. A., H. B. Hellweg, and G. A. O. Davies, "Failure Analysis of Composite Structures Using Interface Elements," Proceedings of the NAFEMS Conference on Application of Finite Elements to Composite Materials, Vol. 1-4, London, U.K., 1997.

44. Schellekens, J. C. J. and R. de Borst, "Numerical Simulation of Free Edge Delamination in Graphite-Epoxy Laminates Under Uniaxial Tension," Proceedings of the 6th International Conference on Composite Structures, 1991, pp. 647-657.

45. Schellekens, J. C. J. and R. de Borst, "On the Numerical Integration of Interface Elements," *International Journal for Numerical Methods in Engineering,* Vol. 36, 1993, pp. 43-66.

46. Wisheart, M. and M. O. W. Richardson, "The Finite Element Analysis of Impact Induced Delamination in Composite Materials Using a Novel Interface Element," *Composites-Part A,* Vol. 28, 1998, pp. 301-313.

47. Daudeville, L., O. Allix, and P. Ladevèze, "Delamination Analysis by Damage Mechanics: Some Applications," *Composites Engineering,* Vol. 5(1), 1995, pp. 17-24.

48. Reeder, J. R., "A Bilinear Failure Criterion for Mixed-Mode Delamination," Composite Materials: Testing and Design, ASTM STP 1206, American Society for Testing and Materials, 1993.

49. Reeder, J. R., "An Evaluation of Mixed-Mode Delamination Failure Criteria," NASA TM 104210, 1992.

50. Cui, W., M. R. Wisnom, and M. Jones, "A Comparison of Failure Criteria to Predict Delamination of Unidirectional Glass/Epoxy Specimens Waisted Through the Thickness," *Composites*, Vol. 23(3), 1992, pp. 158-166.

51. Mohammadi, S., D. R. J. Owen, and D. Peric. "A Combined Finite/Discrete Element Algorithm for Delamination Analysis of Composites," *Finite Elements in Analysis and Design*, Vol. 28(4), 1998, pp. 321-336.

52. Schellekens, J. C. J., "Computational Strategies for Composite Structures," PhD Thesis, Technical University of Delft, The Netherlands, 1992.

53. de Borst, R. and J. G. Rots, "Occurrence of Spurious Mechanisms in Computation of Strain-Softening Solids," *Engineering Computations,* Vol. 6, 1989, pp. 272-280.

54. Alfano, G. and M. A. Crisfield, "Finite Element Interface Elements for the Delamination Analysis of Laminated Composite Structures: Mechanical and Computational Issues", *International Journal for Numerical Methods in Engineering,* Vol. 50, 2001, pp. 1701-1736.

55. Hellweg, H. B., "Nonlinear Failure Simulation of Thick Composites," Ph.D. Thesis, Imperial College of Science and Technology, University of London, U.K., 1994.

56. Riks, E., "An Incremental Approach to the Solution of Snapping and Buckling Problems," *International Journal of Solids and Structures,* Vol. 15, 1975, pp. 529-551.

57. Allix, O., L. Daudeville, and P. Ladevèze, "Delamination and Damage Mechanics," in Mechanics and Mechanisms of Damage in Composites and Multi-Materials, *Mechanical Engineering Publications*, London, U.K., 1991, pp. 143-157.

58. Ladevèze, P., "A Damage Computational Approach for Composites: Basic Aspects and Micromechanical Relations," *Computational Mechanics,* Vol. 17, 1995, pp. 142-150.

59. Allix, O., P. Ladevèze, and D. Lévêque. "Towards a Structural Identification of Delamination Initiation and Growth," Proceedings of the 8th European Conference on Composite Materials, Naples, Italy, 1998, pp. 525-532.

REPORT DOCUMENTATION PAGE

Form Approved
OMB No. 0704-0188

1. AGENCY USE ONLY (Leave blank)	2. REPORT DATE	3. REPORT TYPE AND DATES COVERED
	August 2001	Technical Publication

4. TITLE AND SUBTITLE
Numerical Simulation of Delamination Growth in Composite Materials

5. FUNDING NUMBERS
WU 707-85-10-01

6. AUTHOR(S)
P. P. Camanho, C. G. Dávila, and D. R. Ambur

7. PERFORMING ORGANIZATION NAME(S) AND ADDRESS(ES)
NASA Langley Research Center
Hampton, VA 23681-2199

8. PERFORMING ORGANIZATION REPORT NUMBER
L-18101

9. SPONSORING/MONITORING AGENCY NAME(S) AND ADDRESS(ES)
National Aeronautics and Space Administration
Washington, DC 20546-0001

10. SPONSORING/MONITORING AGENCY REPORT NUMBER
NASA/TP-2001-211041

11. SUPPLEMENTARY NOTES
Camanho: Department of Mechanical Engineering, Faculty of Engineering, University of Porto, Porto, Portugal
Dávila and Ambur: NASA Langley Research Center, Hampton, Virginia

12a. DISTRIBUTION/AVAILABILITY STATEMENT
Unclassified-Unlimited
Subject Category 39 Distribution: Standard
Availability: NASA CASI (301) 621-0390

12b. DISTRIBUTION CODE

13. ABSTRACT (Maximum 200 words)

The use of decohesion elements for the simulation of delamination in composite materials is reviewed. The test methods available to measure the interfacial fracture toughness used in the formulation of decohesion elements are described initially. After a brief presentation of the virtual crack closure technique, the technique most widely used to simulate delamination growth, the formulation of interfacial decohesion elements is described. Problems related with decohesion element constitutive equations, mixed-mode crack growth, element numerical integration and solution procedures are discussed. Based on these investigations, it is concluded that the use of interfacial decohesion elements is a promising technique that avoids the need for a pre-existing crack and pre-defined crack paths, and that these elements can be used to simulate both delamination onset and growth.

14. SUBJECT TERMS
Finite element method; Crack propagation; Fracture mechanics; Composite materials; Debonding

15. NUMBER OF PAGES
24

16. PRICE CODE
A03

17. SECURITY CLASSIFICATION OF REPORT	18. SECURITY CLASSIFICATION OF THIS PAGE	19. SECURITY CLASSIFICATION OF ABSTRACT	20. LIMITATION OF ABSTRACT
Unclassified	Unclassified	Unclassified	UL